

两个氮氧双自由基桥连的稀土一维链的晶体结构、磁性和荧光性能

李弘道* 翟丽军 宋永波 牛宇岚*
(太原工业学院化学与化工系, 太原 030008)

摘要: 选用1,2-二苯氧基乙烷取代的氮氧双自由基(BNPhOEt)与稀土金属反应,得到了2例氮氧双自由基-稀土配合物 $[\text{Ln}(\text{hfac})_3(\text{BNPhOEt})] \cdot \text{C}_6\text{H}_{14}$ (Ln=Tb (**1**), Ho (**2**); hfac=六氟乙酰丙酮), 其均为2*p*-4*f*一维链状结构。磁性研究表明,在配合物**1**和**2**中分别存在铁磁和反铁磁耦合。此外,对2个配合物的荧光光谱进行了研究分析。

关键词: 双自由基; 稀土链; 磁性; 荧光

中图分类号: O614.341; O614.343 文献标识码: A 文章编号: 1001-4861(2021)05-0914-07

DOI: 10.11862/CJIC.2021.113

Two Nitronyl Nitroxide Biradical-Bridged Lanthanide One-Dimensional Chains: Crystal Structure, Magnetic Properties and Luminescent Behavior

LI Hong-Dao* ZHAI Li-Jun SONG Yong-Bo NIU Yu-Lan*

(Department of Chemistry and Chemical Engineering, Taiyuan Institute of Technology, Taiyuan 030008, China)

Abstract: The rational design of 2*p*-4*f* chains, which are made of 4*f* ions and nitronyl nitroxide biradical, has been presented. The reaction of $\text{Ln}(\text{hfac})_3 \cdot 2\text{H}_2\text{O}$ (hfac=hexafluoroacetylacetonate) and nitronyl nitroxide biradical BNPhOEt (BNPhOEt=1,2-(bis-2,2'-(4,4,5,5-tetramethylimidazolyl-1-oxyl-3-oxide) phenoxy)ethane) afforded two isostructural chains of the formula $[\text{Ln}(\text{hfac})_3(\text{BNPhOEt})] \cdot \text{C}_6\text{H}_{14}$ (Ln=Tb (**1**), Ho (**2**)). Direct-current magnetic susceptibility studies show ferromagnetic 4*f*-radical interaction in Tb complex while antiferromagnetic interaction in Ho derivative. In addition, the luminescence emission spectra of two complexes vary depending on lanthanide ion. CCDC: 1906230, **1**; 1906231, **2**.

Keywords: biradical; lanthanide chains; magnetic properties; luminescent behavior

In recent years, rare-earth complexes, exhibiting slow relaxation of magnetization on molecular level, attract a lot of attention on account of their latent adhibition in molecular spintronics and quantum computing^[1-4]. Therefore, great efforts in this field have been devoted to search novel 4*f*-based complexes^[5]. In 2003, Ishikawa and his colleagues obtained the first SMMs (single-molecule-magnets) based on the Tb(III) ion initiating a span-new chapter in molecular magnetism^[6]. More recently, the remarkable magnetic reversal barrier

(U_{eff}) of 1 541 cm^{-1} as well as magnetic hysteresis around 80 K had been achieved with a mononuclear Dy(III) metallocene complex $[(\eta^5\text{-Cp}^*)\text{Dy}(\eta^5\text{-Cp}^{\text{ipr5}})]\text{[B}(\text{C}_6\text{F}_5)_4\text{]}^{[7]}$.

On the other hand, to design and construct Ln-based complexes with diverse structural topologies and intriguing magnetic properties, the option of suitable organic ligands is vital, among which nitronyl nitroxides are very efficient building blocks. Nitronyl nitroxides are very well suited to bind 4*f* ions and provide strong magnetic coupling with lanthanide metal, on

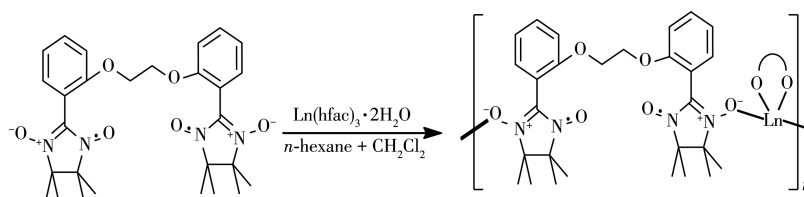
收稿日期: 2020-11-29。收修改稿日期: 2021-04-02。

山西省科技创新项目(No.2020L0650)资助。

*通信联系人。E-mail: lihong.dao@163.com, niuyulan@163.com

account of the direct overlap of orbitals containing unpaired electrons. Accordingly, a number of $4f$ magnetic complexes based on nitronyl nitroxide radicals, including single-chain magnets^[8] and single-molecule magnets^[9], had been reported. For instance, a family of nitronyl nitroxide-lanthanide one-dimensional (1D) chains [Ln(hfac)₃(NITPhOPh)] (Ln=Tb, Dy, Ho, Tm; hfac=hexafluoroacetylacetonate) behave as SCMs (single-chain-magnets)^[10]. Pyridine-substituted nitronyl nitroxide-bridged ring-like Dy-SMMs had been isolated^[11]. In 2010, one tri-spin Dy- nitronyl nitroxide biradical compound, presenting SMM behavior^[12], was synthesized. Previously, we also designed nitronyl nitroxide biradi-

cal (NITPhImbis) bridged 1D lanthanide chains^[13] and two lanthanide complexes involving BNPhOEt biradical [Ln(hfac)₃(BNPhOEt)]·C₆H₁₄ (Ln=Gd, Dy; BNPhOEt=1,2-(bis-2,2'-(4,4,5,5-tetramethylimidazolyl-1-oxyl-3-oxide) phenoxy)ethane)^[14], but the investigation of the coupling between $4f$ ions and radical is limited. Based on this, we continue the above work on nitronyl nitroxide biradical (BNPhOEt) for lucubrating the magnetic coupling between lanthanide metal and nitronyl nitroxide radical and fluorescent properties. Here, we use BNPhOEt ligand to react with Tb (III)/Ho (III) ions for constructing two $4f$ - complexes, namely [Ln(hfac)₃(BNPhOEt)]·C₆H₁₄ (Ln=Tb (**1**), Ho (**2**)) (Scheme 1).



Scheme 1 Schematic representation for synthesis of **1** and **2**

1 Experimental

1.1 Materials and instruments

All reagents are commercially achieved and used without more purification. Elemental analyses (C, H and N) were performed by Perkin-Elmer 240 elemental analyzer. Magnetic measurements were recorded on a Quantum Design SQUID VSM magnetometer. Measured values were corrected for the sample holder and the diamagnetism deduced from Pascal's constants. Fluorescent spectra of complexes **1** and **2** were gathered via F-7000 fluorescence spectrophotometer.

1.2 Syntheses of [Ln(hfac)₃(BNPhOEt)]·C₆H₁₄ (Ln=Tb (**1**), Ho (**2**))

A solution of Ln(hfac)₃·2H₂O (Ln=Tb (**1**), Ho (**2**)) (0.01 mmol) in 16 mL dry *n*-hexane was refluxed for 1.5 h with constant stirring. After cooling to 53 °C, a solution of BNPhOEt (0.0053 g, 0.01 mmol) in CH₂Cl₂ (4 mL) was added in one portion with refluxing for 6 min followed by filtration. The resultant filtrate was left at ambient temperature to evaporate without any disturbance, giving red crystals suitable for X-ray structure analysis over 8 d. For **1**: FT-IR (KBr, cm⁻¹): 1 796(s),

1 358(m), 1 181(s), 1 159(s), 1 074(s), 948(s), 858(m), 547(s) cm⁻¹. Elemental Anal. Calcd for C₄₉H₅₃F₁₈TbN₄O₁₂(%): C, 42.31; H, 3.84; N, 4.03. Found (%): C, 42.05; H, 3.31; N, 3.89. For **2**: FT-IR (KBr, cm⁻¹): 1 795(s), 1 357(m), 1 179(s), 1 160(s), 1 073(s), 947(s), 857(m), 546(s) cm⁻¹. Elemental Anal. Calcd. for C₄₉H₅₃F₁₈HoN₄O₁₂(%): C, 42.13; H, 3.82; N, 4.01. Found (%): C, 42.02; H, 3.49; N, 4.23.

1.3 Crystal structure determination

Crystal data of complexes **1** and **2** were collected at 113(2) K on a Rigaku Saturn CCD diffractometer with Mo *K*α radiation (λ=0.071 073 nm). SADABS^[15] was applied to empirical absorption correction. The structures of two complexes were solved by direct methods and refined by the full-matrix least squares method with a suite of SHELX programs^[16]. Anisotropic parameters were assigned to non-hydrogen atoms. Meanwhile, H atoms were set in calculated positions and refined isotropically by a riding mode. Several severely disordered *n*-hexane molecules in the unit cell of both complexes were treated with SQUEEZE routine^[17] during the structural refinement. Data collection and

refinement parameters are summarized in Table 1, and selected bond distances and bond angles are given in

Table 2 and S1 (Supporting information).

CCDC: 1906230, **1**; 1906231, **2**.

Table 1 Crystallographic data and structure refinement for **1** and **2**

Complex	1	2
Empirical formula	C ₄₉ H ₅₃ F ₁₈ TbN ₄ O ₁₂	C ₄₉ H ₅₃ F ₁₈ HoN ₄ O ₁₂
Formula weight	1 390.70	1 396.71
Crystal system	Trigonal	Trigonal
Space group	$R\bar{3}c$	$R\bar{3}c$
<i>a</i> / nm	3.334 5(6)	3.331 14(16)
<i>b</i> / nm	3.334 5(6)	3.331 14(16)
<i>c</i> / nm	2.424 5(10)	2.428 57(16)
<i>V</i> / nm ³	23.346(13)	23.338(3)
<i>Z</i>	18	18
<i>D_c</i> / (g·cm ⁻³)	1.670	1.679
μ / mm ⁻¹	1.489	1.652
θ range / (°)	3.05~27.54	3.05~27.50
Reflections collected	60 450	79 711
Unique reflection, <i>R_{int}</i>	5 928, 0.080 8	5 801, 0.069 4
GOF (<i>F</i> ²)	1.100	1.055
<i>R</i> ₁ , <i>wR</i> ₂ [<i>I</i> >2 σ (<i>I</i>)]	0.086 7, 0.205 0	0.090 0, 0.215 5
<i>R</i> ₁ , <i>wR</i> ₂ (all data)	0.117 7, 0.225 0	0.116 2, 0.234 7

Table 2 Selected bond lengths (nm) and angles (°) for complexes **1** and **2**

Complex	1	2
Ln—O(rad)	0.232 5(6)	0.230 3(7)
Ln—O(hfac)	0.233 2(6)~0.238 4(5)	0.232 4(7)~0.236 9(7)
O(rad)—Ln—O(rad)	137.7(3)	137.2(3)

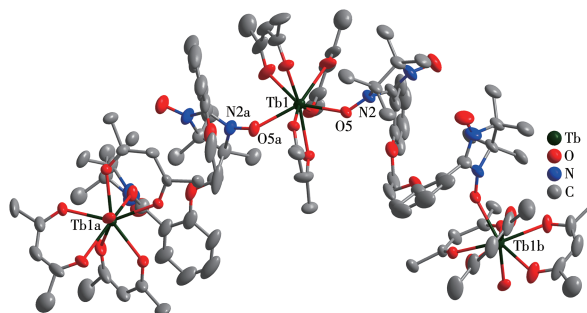
2 Results and discussion

2.1 Description of crystal structures

As revealed by single-crystal X-ray crystallography, complexes **1** and **2** are isostructural and crystallize in the trigonal $R\bar{3}c$ space group. As shown in Fig.1 and S1, each BNPhOEt biradical behaves as a bidentate ligand to bind two Ln(III) ions (Tb(III)/Ho(III)) in the $\mu_2\text{-}\eta^1\text{:}\eta^0\text{:}\eta^0\text{:}\eta^1$ mode via nitroxide groups in the chain. The Ln(III) center is eight-coordinated, surrounded by six oxygen atoms from three chelated hfac⁻ ligands and remaining oxygen atoms descending from nitroxide groups. To determine the coordination sphere of Ln(III) centers, the continuous shape measure parameters (CShMs) were calculated by SHAPE software^[18], indicating the distorted dodecahedron with triangular faces

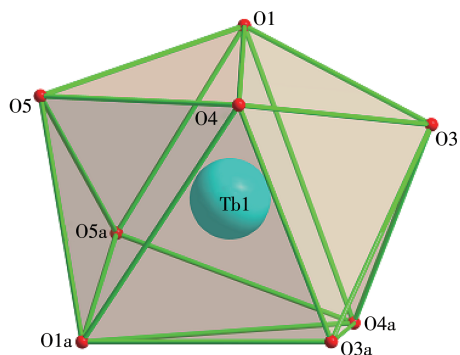
coordination geometry (D_{2d}) for **1** and **2** (Fig.2 and S2, Table 3).

Ln—O_{hfac} bond lengths (0.233 2(6)~0.238 4(5) nm for **1** and 0.232 3(7)~0.237 0(7) nm for **2**) and Ln—O_{radical}



Ellipsoids are set at the 30% probability levels; Hydrogen, fluorine atoms are not shown for clarity; Symmetry codes: a: $-x+4/3, -x+y+2/3, -z+1/6$; b: $y+2/3, x-2/3, -z-1/6$

Fig.1 Crystal structure of complex **1**



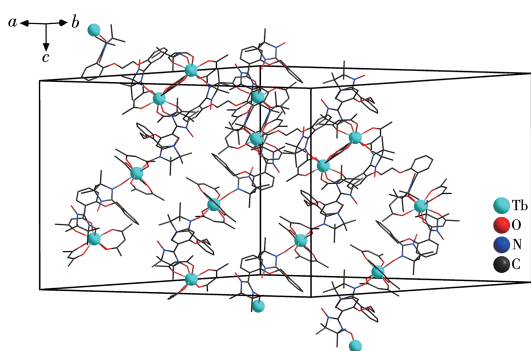
Symmetry code: $a: -x+4/3, -x+y+2/3, -z+1/6$

Fig.2 Local coordination geometry of Tb(III) ion

Table 3 SHAPE analysis for 4f metal of complexes 1 and 2

Complex	TDD-8	BTPr-8	JSD-8
1	0.051	2.570	2.538
2	0.040	2.609	2.568

distances (0.232 5(6) nm for **1** and 0.230 2(7) nm for **2**) are similar to those of reported 4f-radical complexes^[19]. Packing of these chains is shown in Fig.3 and S3. The intrachain distances between both Ln(III) ions are 1.113 nm for **1** and 1.115 nm for **2**, while the nearest interchain Tb...Tb and Ho...Ho separations are found to be 1.094 4 and 1.094 3 nm, respectively. The shortest interchain contacts between uncoordinated nitroxide groups are equal to 0.834 1 and 0.825 1 nm for complexes **1** and **2**, respectively.



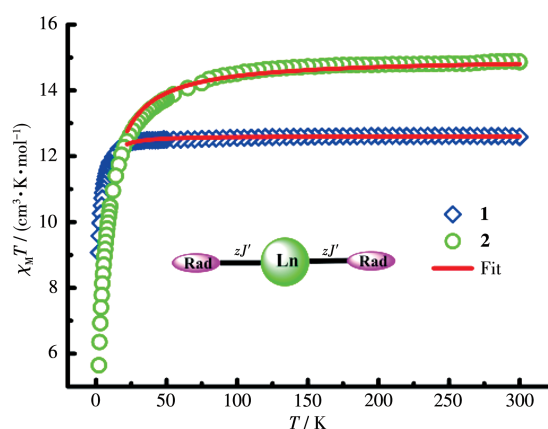
Hydrogen and fluorine atoms are omitted for clarity

Fig.3 Packing diagram of complex **1**

2.2 Magnetic properties

The direct current (dc) magnetic susceptibilities of complexes **1** and **2** were recorded under an external field of 1 000 Oe in a temperature range of 2~300 K. As shown in Fig. 4, the $\chi_M T$ products at 300 K were

12.60 $\text{cm}^3 \cdot \text{K} \cdot \text{mol}^{-1}$ for **1** and 14.85 $\text{cm}^3 \cdot \text{K} \cdot \text{mol}^{-1}$ for **2**, which were slightly higher than theoretical values of 12.57 and 14.82 $\text{cm}^3 \cdot \text{K} \cdot \text{mol}^{-1}$ for one uncoupled Ln(III) ion (Tb(III): 7F_6 , $S=3$, $L=3$, $g=3/2$, $C=11.82 \text{ cm}^3 \cdot \text{K} \cdot \text{mol}^{-1}$; Ho(III): 5I_8 , $S=2$, $L=6$, $g=5/4$, $C=14.07 \text{ cm}^3 \cdot \text{K} \cdot \text{mol}^{-1}$) and one biradical (mono radical: $S=1/2$, $g=2.0$, $C=0.375 \text{ cm}^3 \cdot \text{K} \cdot \text{mol}^{-1}$). For complex **1**, on lowering temperature, the value of $\chi_M T$ stayed relatively unchanged until about 49 K. Then, $\chi_M T$ product fell sharply. For complex **2**, $\chi_M T$ value continuously decreased from room temperature to 5.649 $\text{cm}^3 \cdot \text{K} \cdot \text{mol}^{-1}$ at 2 K.



Solid line represents calculated behavior; Inset: a model of magnetic exchange coupling

Fig.4 $\chi_M T$ vs T plots of complexes **1** and **2**

For both complexes, there are two effective magnetic couplings: (a) the interaction between Tb(III)/Ho(III) ion and coordinated nitroxide group; (b) magnetic coupling between both NO groups through Tb(III)/Ho(III) ion. The magnetic interaction between two mono-radicals within the biradical is expected to be very weak. To achieve a rough quantitative analysis, based on the large anisotropy of Tb(III) and Ho(III), we suppose that the total magnetic susceptibility (χ_{total}) is the aggregation of the isolated lanthanide ion and two mono-radicals (Eq. 1). Tb(III)/Ho(III) ion may be assumed to show a splitting of the m_j energy levels in an axial crystal field^[20]. Δ represents the zero-field-splitting parameter. Thus, Eq. 2~4 can be used to describe χ_{Tb} , χ_{Ho} and χ_{rad} , respectively. The magnetic coupling between 4f ion and mono-radical is introduced by the mean-field, zJ' (Eq.5).

$$\chi_{\text{total}} = \chi_{\text{Ln}} + 2\chi_{\text{rad}} \quad (1)$$

$$\chi_{\text{Tb}} = \frac{2Ng^2\beta^2}{kT} \left[\frac{36\exp\left(\frac{-36\Delta}{kT}\right) + 25\exp\left(\frac{-25\Delta}{kT}\right) + 16\exp\left(\frac{-16\Delta}{kT}\right) + 9\exp\left(\frac{-9\Delta}{kT}\right) + 4\exp\left(\frac{-4\Delta}{kT}\right) + \exp\left(\frac{-\Delta}{kT}\right)}{2\exp\left(\frac{-36\Delta}{kT}\right) + 2\exp\left(\frac{-25\Delta}{kT}\right) + 2\exp\left(\frac{-16\Delta}{kT}\right) + 2\exp\left(\frac{-9\Delta}{kT}\right) + 2\exp\left(\frac{-4\Delta}{kT}\right) + 2\exp\left(\frac{-\Delta}{kT}\right) + 1} \right] \quad (2)$$

$$\chi_{\text{Ho}} = \frac{2Ng^2\beta^2}{kT} \left[\frac{64\exp\left(\frac{-64\Delta}{kT}\right) + 49\exp\left(\frac{-49\Delta}{kT}\right) + 36\exp\left(\frac{-36\Delta}{kT}\right) + 25\exp\left(\frac{-25\Delta}{kT}\right) + 16\exp\left(\frac{-16\Delta}{kT}\right) + 9\exp\left(\frac{-9\Delta}{kT}\right) + 4\exp\left(\frac{-4\Delta}{kT}\right) + \exp\left(\frac{-\Delta}{kT}\right)}{2\exp\left(\frac{-64\Delta}{kT}\right) + 2\exp\left(\frac{-49\Delta}{kT}\right) + 2\exp\left(\frac{-36\Delta}{kT}\right) + 2\exp\left(\frac{-25\Delta}{kT}\right) + 2\exp\left(\frac{-16\Delta}{kT}\right) + 2\exp\left(\frac{-9\Delta}{kT}\right) + 2\exp\left(\frac{-4\Delta}{kT}\right) + 2\exp\left(\frac{-\Delta}{kT}\right) + 1} \right] \quad (3)$$

$$\chi_{\text{rad}} = \frac{Ng_{\text{rad}}^2\beta^2}{3kT} \frac{1}{2} \left(\frac{1}{2} + 1 \right) \quad (g_{\text{rad}} = 2) \quad (4)$$

$$\chi_{\text{M}} = \frac{\chi_{\text{total}}}{1 - [2zJ'/(Ng^2\beta^2)]\chi_{\text{total}}} \quad (5)$$

The best fitting parameters $g=1.51$, $\Delta=0.11 \text{ cm}^{-1}$, $zJ'=0.022 \text{ cm}^{-1}$ were given for complex **1** in a range of 20~300 K and the determined zJ' value manifests that

there is ferromagnetic interaction between Tb(III) ion and the coordinated mono-radical. For **2**, $g=1.26$, $\Delta=-0.02 \text{ cm}^{-1}$, $zJ'=-0.06 \text{ cm}^{-1}$ in the same temperature range. The negative value of zJ' indicates the antiferromagnetic Ho(III)-radical interaction. These values are consistent with values previously observed for Ln-rad complexes^[21] (Table 4).

Table 4 Magnetic parameters for Ln-rad complexes with tri-spin units

Complex	zJ' / cm^{-1}	Δ / cm^{-1}	Ref.
[Tb(hfac) ₃ (NITNapOMe) ₂]	0.26	0.55	[21a]
[Tb(hfac) ₃ (NITPhSCF ₃) ₂]	0.024	0.051	[21b]
[Tb(hfac) ₃ (NITPh-3-Br-4-OMe) ₂]	-0.09	-0.19	[21c]
[Tb(hfac) ₃ (BNPhOEt)]·C ₆ H ₁₄	0.022	0.11	This work
[Ho(hfac) ₃ (NITNapOMe) ₂]	-0.05	-0.03	[21a]
[Ho(hfac) ₃ (NITPh-3-Br-4-OMe) ₂]	-0.04	-0.02	[21c]
[Ho(hfac) ₃ (BNPhOEt)]·C ₆ H ₁₄	-0.06	-0.02	This work

The magnetization as a function of applied field was determined at 1.8 K in a field range of 0~70 kOe (Fig. 5). The M versus H plots of complexes **1** and **2** displayed that M values increased precipitously at low fields, then the magnetization increased gently and did not reach saturation values at 70 kOe. The behavior of both complexes manifests the presence of low-lying

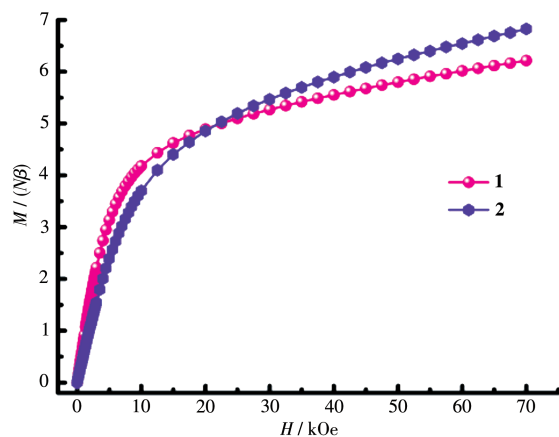


Fig.5 Field dependence of magnetization at 2 K for complexes **1** and **2**

excited states and/or significant magnetic anisotropy.

To study the dynamic magnetism of complex **1**, temperature-dependent alternating-current (ac) susceptibility data were collected, but no out-of-phase signal could be observed under zero direct-current (dc) field (Fig.6). To restrain possible quantum tunneling process (QTM), 3 kOe dc field was applied to probe dynamic

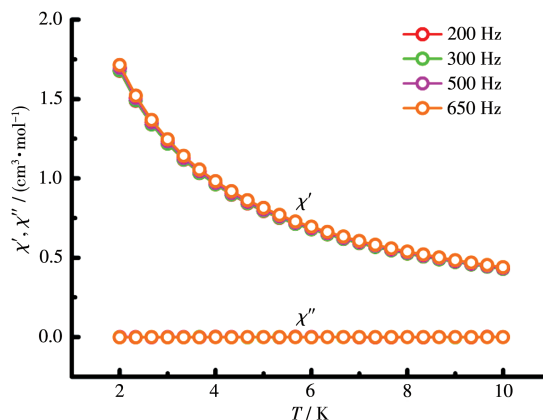


Fig.6 Temperature dependence of in-phase and out-of-phase of ac magnetic susceptibilities for **1** in zero dc field with an oscillation of 3 Oe

magnetic behavior. As depicted in Fig.S5, the out-of-phase susceptibility curves showed weak frequency dependent, revealing the presence of slow relaxation magnetization.

2.3 Fluorescent properties

The fluorescent spectra of Tb and Ho complexes in CH_2Cl_2 ($10 \mu\text{mol}\cdot\text{L}^{-1}$) was researched at room temperature. Characteristic fluorescent emissive peaks of Tb(III) ion were observed with four narrow emission

bands at 491, 547, 581 and 622 nm, which correspond to the $^5D_4\text{-}^7F_6$, $^5D_4\text{-}^7F_5$, $^5D_4\text{-}^7F_4$ and $^5D_4\text{-}^7F_3$ transitions of Tb(III) ion. The stronger emission intensity of the $^5D_4\text{-}^7F_5$ transition manifests that biradical BNPhOEt is propitious to sensitize green light of Tb(III) ion (Fig. 7, left). Complex **2** displayed emission spectra at 339, 411 and 470 nm, assigned to the characteristic emission of the $^5I_8\text{-}^5G_4\text{+}^3F_7$ transition of the Ho^{3+} center^[22] (Fig.7, right).

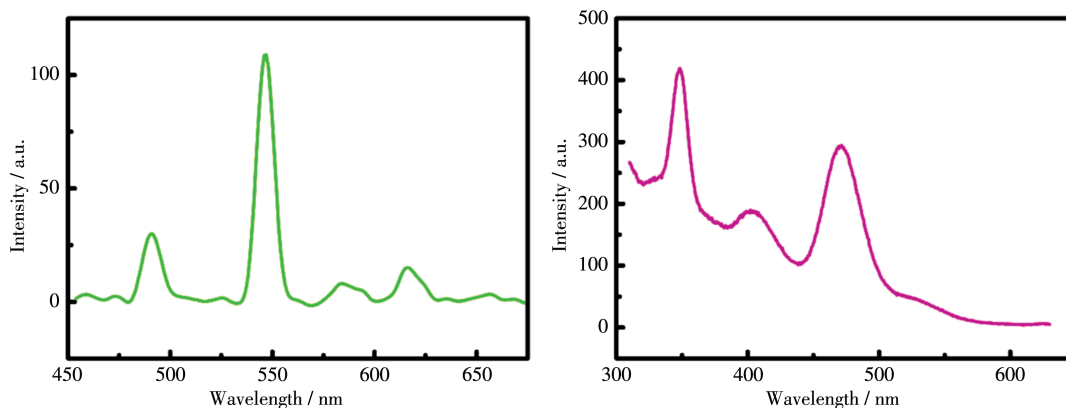


Fig.7 Emission spectra of complexes **1** (left) and **2** (right)

3 Conclusions

In summary, two one-dimensional biradical-bridged lanthanide complexes $[\text{Ln}(\text{hfac})_3(\text{BNPhOEt})] \cdot \text{C}_6\text{H}_{14}$ ($\text{Ln}=\text{Tb}$ (**1**), Ho (**2**)) have been successfully designed and synthesized, in which $4f$ ions are connected by biradical ligands through the NO groups of two mono-radicals. The magnetic studies indicate that there are ferromagnetic $4f$ -radical coupling in **1** and antiferromagnetic interaction in **2**. Tb complex displayed slow relaxation magnetization. Moreover, the fluorescent emission spectra of $[\text{Ln}(\text{hfac})_3(\text{BNPhOEt})] \cdot \text{C}_6\text{H}_{14}$ exhibited typical $4f$ -centered luminescence. This work not only enables us to understand the optical behavior and magnetic interactions between lanthanide ion and nitronyl nitroxide radical, but also provides valuable insight into the chemistry of $2p\text{-}4f$ complexes.

Acknowledgements: This work was supported by Science and Technology Innovation Project of Shanxi Province (Grant No.2020L0650).

Supporting information is available at <http://www.wjhx.cn>

References:

- [1] (a)Dossantos C, Harte A, Quinn S, Gunnlaugsson T. *Coord. Chem. Rev.*, **2008**,**252**:2512-2527
(b)Wang X D, Wolfbeis O S, Meier R J. *Chem. Soc. Rev.*, **2013**,**42**: 7834-7869
(c)Silvi S, Credi A. *Chem. Soc. Rev.*, **2015**,**44**:4275-4289
- [2] Wernsdorfer W, Aliaga N A, Hendrickson D N, Christou G. *Nature*, **2002**,**416**:406-409
- [3] (a)Wernsdorfer W, Sessoli R. *Science*, **1999**,**284**:133-135
(b)Bogani L, Wernsdorfer L B. *Nat. Mater.*, **2008**,**7**:179-186
- [4] Hill S, Edwards R S, Aliaga N A, Christou G. *Science*, **2003**,**302**:1015-1018
- [5] (a)Guo Y N, Xu G F, Gamez P, Zhao L, Lin S Y, Deng R, Tang J K, Zhang H J. *J. Am. Chem. Soc.*, **2010**,**132**:8538-8539
(b)Roy J J L, Ungur L, Korobkov I, Chibotaru L F, Murugesu M. *J. Am. Chem. Soc.*, **2014**,**136**:8003-8010
(c)Qin L, Singleton J, Chen W P, Nojiri H, Engelhardt L, Winpenny R E P, Zheng Y Z. *Angew. Chem. Int. Ed.*, **2017**,**56**:16571-16574
(d)Daniel N W, Richard A L, Richard E P W. *Chem. Rev.*, **2013**,**113**: 5110-5148
(e)Lu J J, Guo M, Tang J K. *Chem. Asian J.*, **2017**,**12**:2772-2779
- [6] Ishikawa N, Sugita M, Ishikawa T, Koshihara S Y, Kaizu Y. *J. Am. Chem. Soc.*, **2003**,**125**:8694-8695
- [7] Guo F S, Day B M, Chen Y C, Tong M L, Mansikkamäki A, Layfield R A. *Science*, **2018**,**362**:1400-1403

- [8] (a) Han T, Shi W, Niu Z, Na B, Cheng P. *Chem. Eur. J.*, **2013**,**19**:994-1001
(b) Liu R N, Li L C, Wang X L, Yang P P, Wang C, Liao D Z, Sutter J P. *Chem. Commun.*, **2010**,**46**:2566-2568
(c) Yang M, Xie J, Sun Z, Li L C, Sutter J P. *Inorg. Chem.*, **2017**,**56**:13482-13490
(d) Liu X Q, Zhang Y, Shi W, Cheng P. *Inorg. Chem.*, **2018**,**57**:13409-13414
- [9] (a) Zhou N, Ma Y, Wang C, Xu G F, Tang J K, Xu J X, Yan S P, Cheng P, Li L C, Liao D Z. *Dalton Trans.*, **2009**,**40**:8489-8492
(b) Coronado E, Saiz C G, Recuenco A, Tarazón A, Romero F M, Camón A, Luis F. *Inorg. Chem.*, **2011**,**50**:7370-7372
(c) Lv X H, Yang S L, Lia Y X, Zhang C X, Wang Q L. *RSC Adv.*, **2017**,**7**:38179-38186
(d) Chen P Y, Wu M Z, Li T, Shi X J, Tian L, Liu Z Y. *Inorg. Chem.*, **2018**,**57**:12466-12470
- [10] (a) Bogani L, Sangregorio C, Sessoli R, Gatteschi D. *Angew. Chem., Int. Ed.*, **2005**,**44**:5817-5821
(b) Bernot K, Bogani L, Caneschi A, Gatteschi D, Sessoli R. *J. Am. Chem. Soc.*, **2006**,**128**:7947-7956
- [11] Poneti G, Bernot K, Bogani L, Caneschi A, Sessoli R, Wernsdorfer W, Gatteschi D. *Chem. Commun.*, **2007**,**18**:1807-1809
- [12] Bernot K, Pointillart F, Rosa P, Etienne M, Sessoli R, Gatteschi D. *Chem. Commun.*, **2010**,**46**:6458-6460
- [13] Li H D, Sun J, Yang M, Sun Z, Xie J, Ma Y, Li L C. *New J. Chem.*, **2017**,**41**:10181-10188
- [14] Li H D, Guo J N, Sun G F, Xie J, Li L C. *Inorg. Chem. Commun.*, **2017**,**85**:62-65
- [15] Sheldrick G M. *SADABS*, University of Göttingen, Germany, **2011**.
- [16] (a) Sheldrick G M. *SHELXS - 2014, Program for the Solution of Crystal Structures*, University of Göttingen, Germany, **2014**.
(b) Sheldrick G M. *SHELXL-2014, Program for the Structure Refinement of Crystal Structures*, University of Göttingen, Germany, **2014**.
- [17] Spek A L. *Acta Crystallogr. Sect. D*, **2009**,**D65**:148-155
- [18] (a) Casanova D, Llunell M, Alemany P, Alvarez S. *Chem. Eur. J.*, **2005**,**11**:1479-1494
(b) Llunell M, Casanova D, Cirera J, Alemany P, Alvarez S. *SHAPE 2.1*, University of Barcelona, Spain, **2013**.
- [19] (a) Li L L, Liu S, Zhang Y, Shi W, Cheng P. *Dalton Trans.*, **2015**,**44**:6118-6125
(b) Xiao Z X, Miao H, Shao D, Wei H Y, Zhang Y Q, Wang X Y. *Chem. Commun.*, **2018**,**54**:9726-9729
(c) Sun P P, Yang S L, Zhang C X, Wang Q L. *Polyhedron*, **2018**,**156**:155-160
- [20] (a) Xu J X, Ma Y, Liao D Z, Xu G F, Tang J K, Wang C, Zhou N, Yan S P, Cheng P, Li L C. *Inorg. Chem.*, **2009**,**48**:8890-8896
(b) Xu N, Wang C, Shi W, Yan S P, Cheng P, Liao D Z. *Eur. J. Inorg. Chem.*, **2011**,**15**:2387-2393
(c) Ouyang Y, Zhang W, Xu N, Xu G F, Liao D Z, Yoshimura K, Yan S P, Cheng P. *Inorg. Chem.*, **2007**,**46**:8454-8456
- [21] (a) Wang Y L, Gao Y Y, Ma Y, Wang Q L, Li L C, Liao D Z. *CrystEngComm*, **2012**,**14**:4706-4712
(b) Song M Y, Hou Y F, Wen L M, Wang S P, Yang S T, Zhang J J, Geng L N, Shi S K. *J. Mol. Struct.*, **2016**,**1107**:174-181
(c) Wang Y L, Gao Y Y, Ma Y, Wang Q L, Li L C, Liao D Z. *J. Solid. State Chem.*, **2013**,**202**:276-281
- [22] Feng X, Li S H, Wang L Y, Zhao J S, Shi Z Q, Lei P P. *CrystEngComm*, **2012**,**14**:3684-3693